Phase Jump Due to Partial Reflection of Irregular Water Waves at Steep Slopes

By Fritz Büsching

urn:nbn:de:0066-201011099

Summary

A wave pulse of transmission originating at the landward side of the initial breaking wave requires the simultaneous formation of a reflected wave at the seaward side. According to the conservation of momentum the water level deflection of the reflected wave must be negative. Superimposition of incident and reflected waves results in the formation of a partial standing wave (partial clapotis) comprising of a phase jump.

For the investigation of partial standing waves at steep sloping structures a special analyzing technique had been adopted. Previous results on the phenomenon of anomalous dispersion and on frequency dependent reflections are summarized and are supplemented by evaluations on the existence of phase jumps between incident and reflected waves: The nodes of superimposing partial clapotis component waves nearest to a smooth structure are very close to the point of intersection (IP), where the still water level intersects the face of the structure. Such a partial reflection, assigned by a phase jump of $\Delta\varphi \approx 180°$, leads to the definition of a negative coefficient of reflection $C_r = f(H_r/H_i, \Delta\varphi) < 0$, implying the effect that a wave crest is reflected by a wave trough and vice versa. Structured (rough) surfaces (like hollow revetments or big hollow blocks) cause phase differences $\Delta\varphi < 180°$ between incident and reflected waves together with reflection coefficients ranging between $C_r < +1{,}0$ and $C_r > -1{,}0$. Minimal magnitudes of reflection coefficients $C_r = f(H_r/H_i, \Delta\varphi)$ are found for phase differences $\Delta\varphi \approx 90°$.

Zusammenfassung

Eine im Verlauf des Wellenbrechvorganges landseitig entstehende Transmissionswelle mit der Phasengeschwindigkeit $c_t < c_i$ erfordert aus Gründen der Impulserhaltung seeseitig die gleichzeitige Bildung einer Reflexionswelle mit örtlich negativer Wasserspiegelauslenkung. Die Überlagerung der anlaufenden mit der reflektierten Welle ergibt eine partielle Clapotis mit Phasensprung.

Für die Untersuchung partiell stehender Wellen an steilen Uferböschungen im Modellmaßstab 1:5 wurde auf entsprechende Messungen eine spezielle spektrale Analysetechnik angewandt. Auf dieser Grundlage gewonnene frühere Ergebnisse zum Phänomen anomaler Dispersion und frequenzabhängiger Reflexion werden zusammengefasst und durch neue Auswertungen im Hinblick auf das Vorliegen von Phasensprüngen ergänzt: Die bauwerksnahsten imperfekten Knoten eines Kollektivs partiell stehender Wellen (Partialwellen) vor glatten Böschungen befinden sich in unmittelbarer Nähe des Schnittpunktes, den der Ruhewasserspiegel mit der Böschungsoberfläche bildet. Eine dementsprechende partielle Reflexion mit einem Phasensprung $\Delta\varphi \approx 180°$ führt zur Definition negativer Reflexionskoeffizienten $C_r = f(H_r/H_i, \Delta\varphi) < 0$ mit der Folge, dass ein Wellenberg als Wellental reflektiert wird und umgekehrt.

Strukturierte (raue) Oberflächen (wie Hohldeckwerke einerseits und großvolumige Hohlformkörper andererseits) bewirken Phasendifferenzen $\Delta\varphi < 180°$ zwischen anlaufenden und reflektierten Wellen mit Reflexionskoeffizienten zwischen $C_r < +1{,}0$ und $C_r > -1{,}0$.

Minimale Beträge des Reflexionskoeffizienten $C_r = f(H_r/H_i, \Delta\varphi)$ ergeben sich für die Phasendifferenzen $\Delta\varphi \approx 90°$.

Keywords

Phase jump, reflection coefficient, partial standing wave, partial clapotis, wave breaking, revetment, hollow cubes, wave spectrum, anomalous dispersion.

Contents

1. Introduction

In the 1990ies numerous model investigations had been carried out in a wave tank at Bielefeld University of Applied Sciences (BUAS) in order to demonstrate the hydraulic efficiency of hollow revetment elements (Hollow Cubes) using a model scale 1:5, see Fig.1. In doing so the author started from the perception that the mass of water in front of a sloping structure can be regarded as an oscillating continuum, characterized by different natural frequencies, according to the actual geometric boundaries.

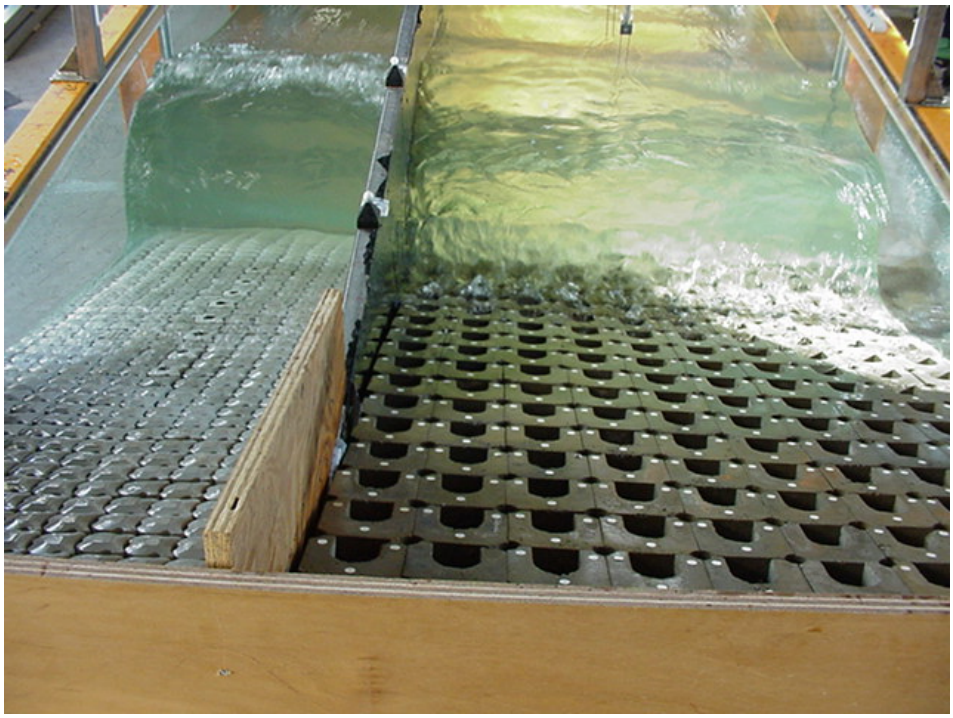

Fig. 01: Plunging breaker at quasi smooth reference revetment slope (left) and collapsing breaker at hollow slope structure (right)

In this arrangement the source of excitation is realised in the waves coming from the sea and the different degrees of freedom are represented – on the one hand - by the reflections associated with a set of partial standing waves and - on the other hand – by the washing movement due to run-up and run-down of broken waves on the slope face [1]. Actually it could be shown that the appropriate interferences on the washing movements not only have the effect of reducing the wave run-up but also reducing the breaker heights, changing the breaker type and changing its relative position on the slope face. Contrary to that the present contribution is oriented a priori on the partial clapotis, namely on the phase difference between incident and reflected wave occurring in the course of partial reflection at sloping structures. This subject is important, because erosions at the slope face and scouring at the foot of coastal structures are due to the interaction of incident and reflected waves. Although the effect of phase shifting had yet been presumed by Schoemaker und Thijsse (1949) [2], relatively little attention had been paid on it during the years 1980 to 2000, when the relevant studies on reflection coefficients C_r had been carried out. Sutherland and O'Donoghue (1998) [4] analyzed the state of knowledge from about 20 references complimenting it by their own measurements. Using a large experimental data set involving normally incident and obliquely incident regular and irregular waves, they show that the phase shift γ is uniquely determined by a nondimensional number χ_3 defined by structure slope $\tan\alpha = 1{:}m$, water depth at the structure toe d_t, wave period T, and angle of incidence θ:

$$\chi_3 = \chi\sqrt{\cos\theta} = \frac{1}{\tan\alpha}\sqrt{\frac{d_t\cos\theta}{gT^2}}\,. \qquad (1)$$

Accordingly neither the wave height nor energy dissipation processes should influence the phase shift γ.
In total the authors give 2 theoretical linear functions $\gamma = f(\chi)$ for normal wave incidence and 5 experimental power functions $\gamma = f(\chi)$ and $\gamma = f(\chi 3)$ respectively applying to 2- and 3-dimensional regular and irregular waves. For instance that one for 3-dimensional irregular waves reads as follows:

$$\gamma = -11.13 \cdot \pi \cdot \chi_3^{1,41} \qquad (2)$$

Here the point of origin is x = 0 at the structure toe with x increasing toward the shore. This applies to the very most investigations including those by Kobayashi, Tomasiccho and Brunone (2000) [14], who analyzed co-located measurements of the free surface elevation and horizontal velocity.
For the time being, however, relations to the above studies can not be made, because in the present assessment

- the point IP of the still water level intersecting the slope face is selected as the point of reference and thus the phase shift here is $\Delta\varphi \neq \gamma$,
- the investigations are restricted to the 2-dimesional retro-reflection from 2 steep slopes only,
- contrary to above presumptions *essential importance* is attached to the interactions between phase shift and energy dissipation at wave breaking and
- absorption at sloping structures is assumed to be not only represented by a smaller reflecting wave height $H_r < H_i$ but also is accompanied by a modified phase shift between incident and reflected wave.

The summary of the results may be anticipated yet at this point as follows:
At steep plane slopes wave breaking not only causes dissipation and reflection but transmission also.
Accordingly a phenomenological representation can be described by the following:
In the course of the dissipative wave breaking process a wave pulse of transmission evolves from the initial incident wave at the landward side, while a reflected wave is produced at the seaward side at the same time.
The wave pulse of transmission is characterized by a wave height $H_t < H_i$ and phase velocity $c_t < c_i$, and the reflected wave height is $H_r < H_i$.
In this process it is essential that due to conservation of momentum the positive water level deflection of the transmitted wave pulse postulates locally a negative water level deflection at the reflecting wave. Hence, superimposition of incident and reflected waves results in a partially standing wave comprising of a phase jump. The partial clapotis node close to IP can be looked upon as a centre of rotation, around which the water level deflections of the washing movement (run-up – rundown) and those of the partial standing wave are in opposite phases.

German versions of this publication can be found in [15].

2. M e t h o d

The investigations are based on measurements which had been carried out in the BUAS wave tank. As the method used for spectral data analysis may not be well-established, in the following the results achieved will be summarized with respect to the topic of reflection at inclined coastal structures with slopes 1:m = 1:3 and 1:2.
Particular attention is paid, however, on the process of reflection at a *smooth* inclined slope, which had been used as a reference slope for the respective investigations, see Fig. 2.

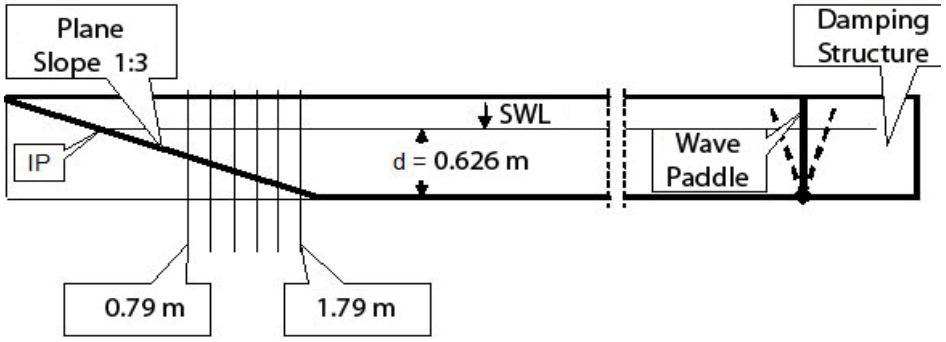

Fig. 02: Scheme of BUAS Wave Tank (not to scale).

Due to the water depth conditions to be considered in the wave flume, an input wave spectrum was used similar to those measured near the breaker zone of Sylt Island/North Sea [5]. Hence in the model input spectrum maximum energy densities are concentrated in the frequency range 0.48 Hz ≤ f ≤ 0.62Hz.
The actual evaluations refer to the boundary conditions of a smooth slope inclined 1:3 and a rigid flap type wave generator. In order to favour the development of high energetic movements in the tank (with wave heights of about 0.35m), in this case, no precautions had been made to suppress *re-reflection* from the wave maker. The tests had been carried out comprising a rather big number of 91 wave probe stations positioned in front of the slope from station 0.79m to 9.79m, equally spaced 10cm, nearly all over the total length of the wave tank. The signals from the wave probes were recorded quasi synchronously and were processed by spectrum analyses confined to a total frequency range 0.03263 ≤ f ≤ 1.3997 Hz.

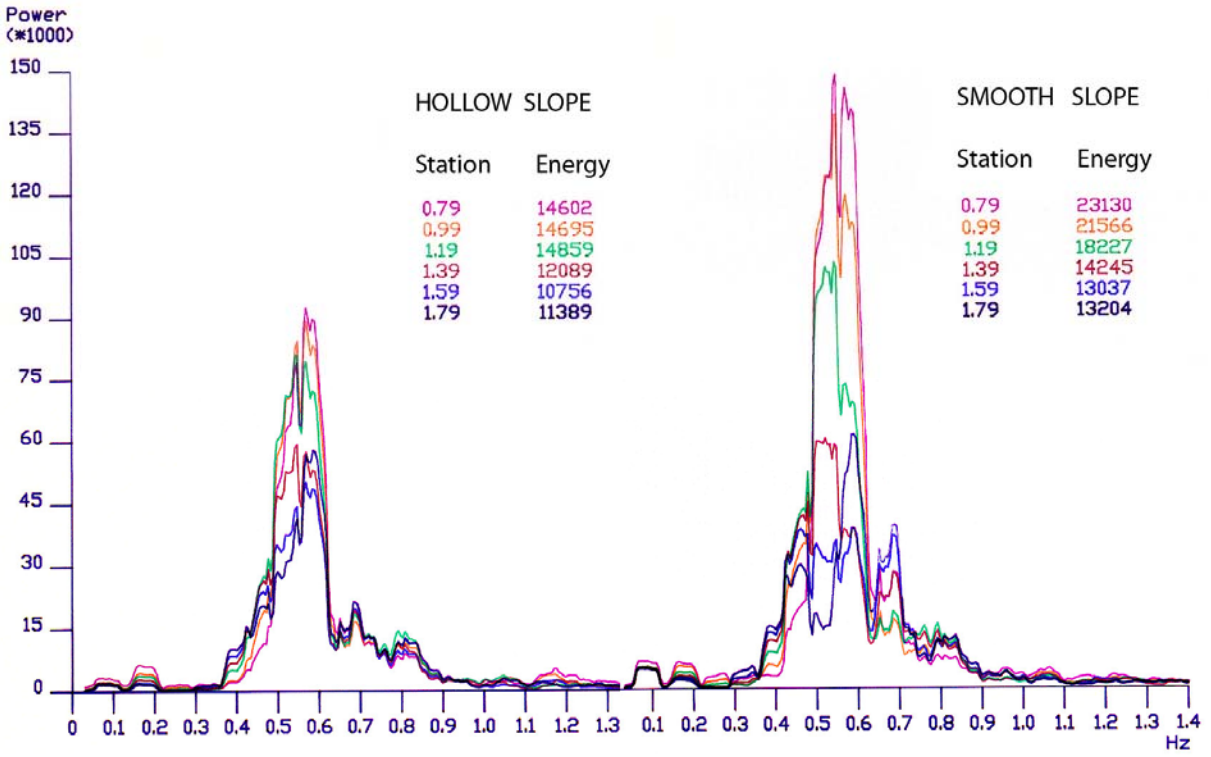

Fig. 03. Synchronously measured energy spectra at stations 0.79m to 1.79m distant from IP. In front of a Hollow Revetment (left) and a Plane Revetment Structure (right) at Slopes 1:3.

As an example Fig.03 shows plots of spectra synchronously taken at 6 different gage locations, spaced 20cm, in front of the hollow slope and the plane slope respectively. Actually those *composite* energy spectra (containing information of incident waves, reflected waves and re-reflected waves) demonstrate the changes of energy content along the slope in the range extending from the slope toe (station 1.79m) to the zone of maximum breaker instability (stations 1.19m to 0.79m).

Due to the fact that the area included in each of the energy spectra (integrated spectrum area, IA) is proportional to the potential energy at any measuring station, such values were used in order to describe the distribution of the energy along the wave flume with reference to different frequency ranges.

In the 3 diagrams attached (Fig.04 to Fig.06) the values of all the integrated spectra IA are plotted along with the gauge station distance from the slope face, i.e., from the point IP of the still water level (SWL) intersecting the slope, which is also sketched in relation to the probe stations at the bottom of Fig.04.

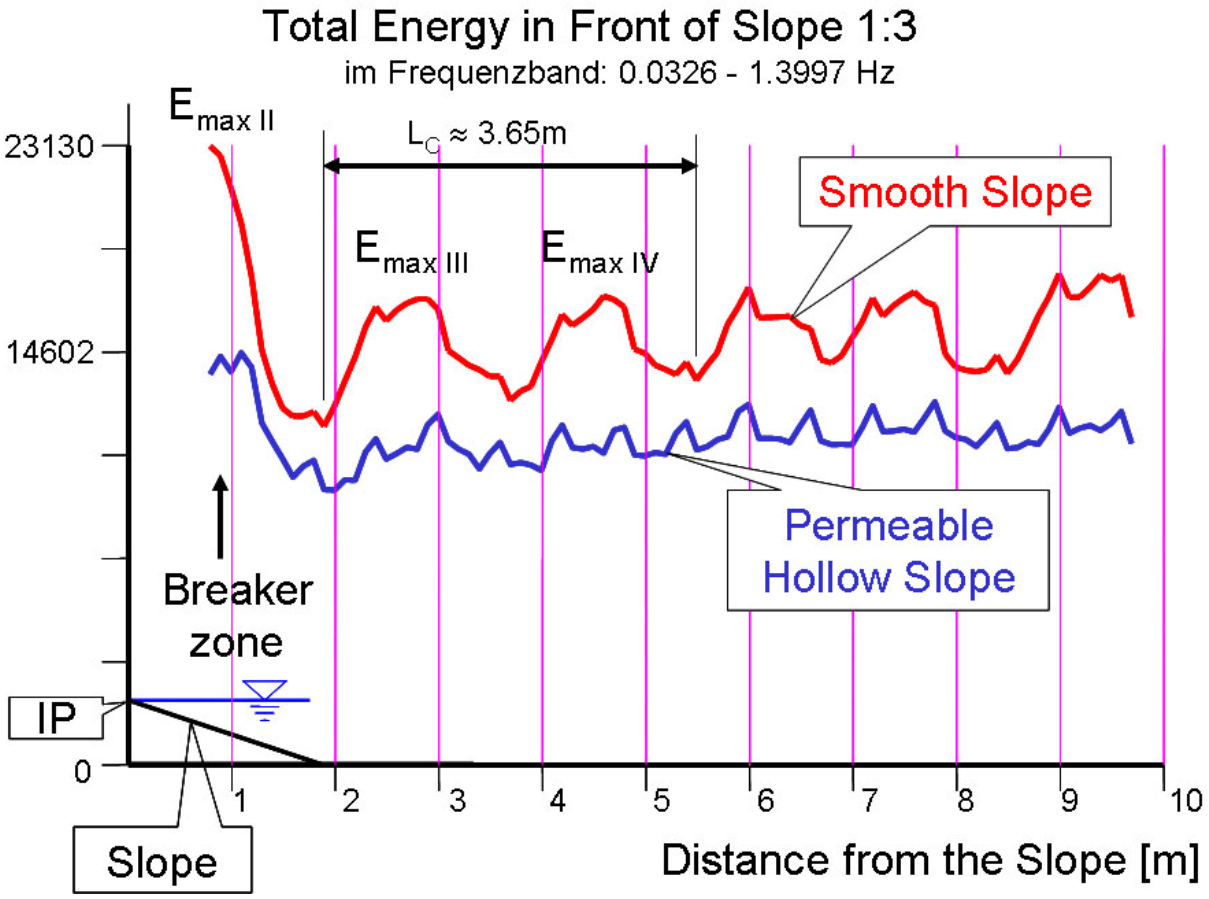

Fig. 04: Distribution of spectral energy (within the frequency range $0.03 \leq f \leq 1.4$ Hz) documenting the existence of a partial clapotis in front of the smooth slope 1:3 (red curve).

With respect to the total analyzed frequency range $0.0326\text{Hz} \leq f \leq 1.3997\text{Hz}$ a *periodic feature* can be noticed yet in the upper red curve, which belongs to the potential energy data calculated for the *smooth* sloping structure in Fig.4.
This feature apparently confirms the existence of a partial standing wave, because the potential energy of such a wave – contrary to a progressive wave – keeps on location. Its wave length of about $L_C = 3.65$m for instance can be taken from the graph to be equal to the distance between the first and third minimum of energy.
Although there are some disturbances to be seen in the plot, it will be shown that conclusions of good quality can be drawn from that data, provided that the total frequency range is subdivided into a number of smaller frequency ranges and the higher noise frequencies ($f > 0.8$Hz) are discarded.

First of all in Fig.05 a respective presentation of all the frequency components *separately* (82 spaced $\Delta f = 0.00543$ Hz) is shown for the frequency range $0.4015\text{Hz} \leq f \leq 0.8409$ Hz. The *essential* phenomenon to be seen from this graph consists in the fact that obviously there are

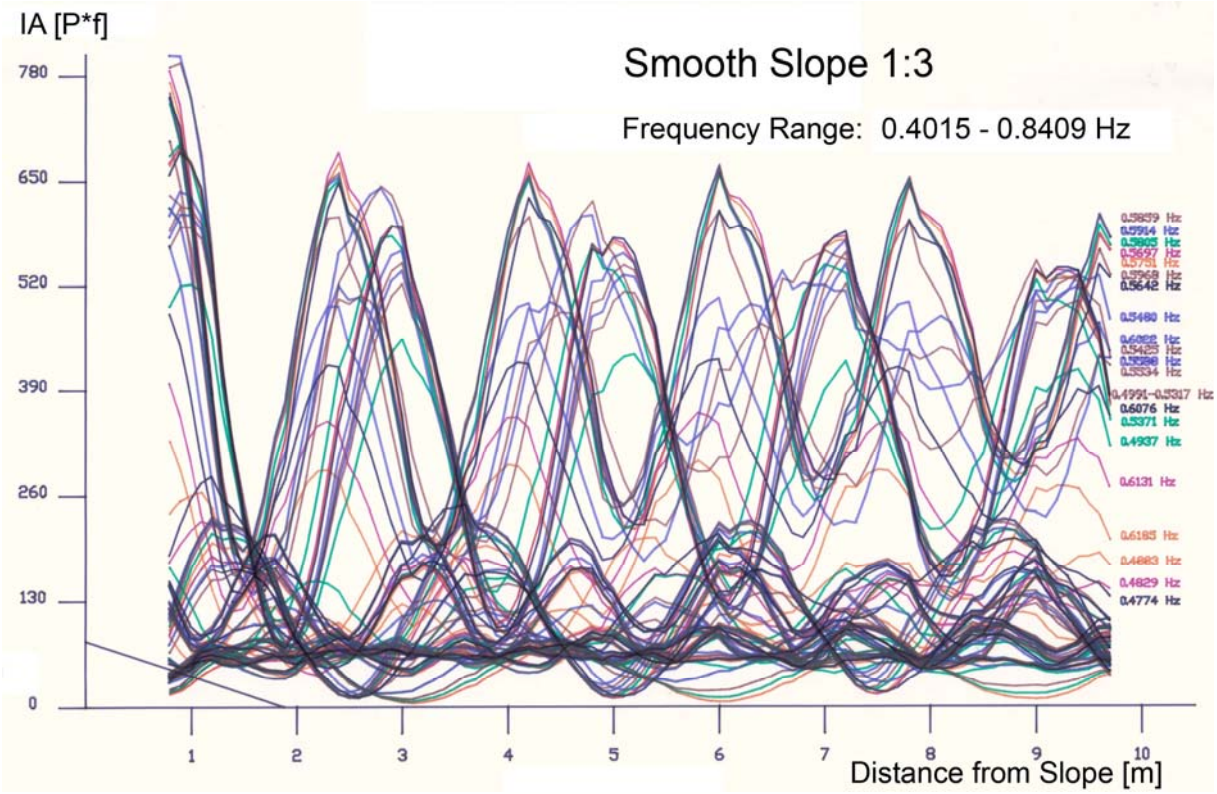

Fig. 05: Energy lines of all the components in the frequency range $0.4015\text{Hz} \leq f \leq 0.8409\ \text{Hz}$.

lines of energy, possessing *similar* energy distributions in the length expansion, relating to the distance from the sloping structure (point IP); i.e., they have nearly same distances between neighbouring energy minima or neighbouring energy maxima respectively and nearly same phase angles too.

In the course of further data treatment the energy components of such similar neighbouring frequency ranges had been summed up reducing the number of curves. Thus in the frequency range of $0.4015\text{Hz} \leq f \leq 0.8030\text{Hz}$, see Fig.06, 12 curves were found, representing different component frequency ranges. Hence, the potential energy of the partial clapotis, documented in Fig.04, can be recognized approximately as the resulting energy from such 12 superimposing partial clapotis waves existing in the wave tank at the same time. In order to distinguish the resultant partial clapotis from its components in the following the latter shall be named shortly "partial waves".

The general properties of such partial waves can be derived from their energy distribution in the length expansion (energy line) as shown in Fig.07.

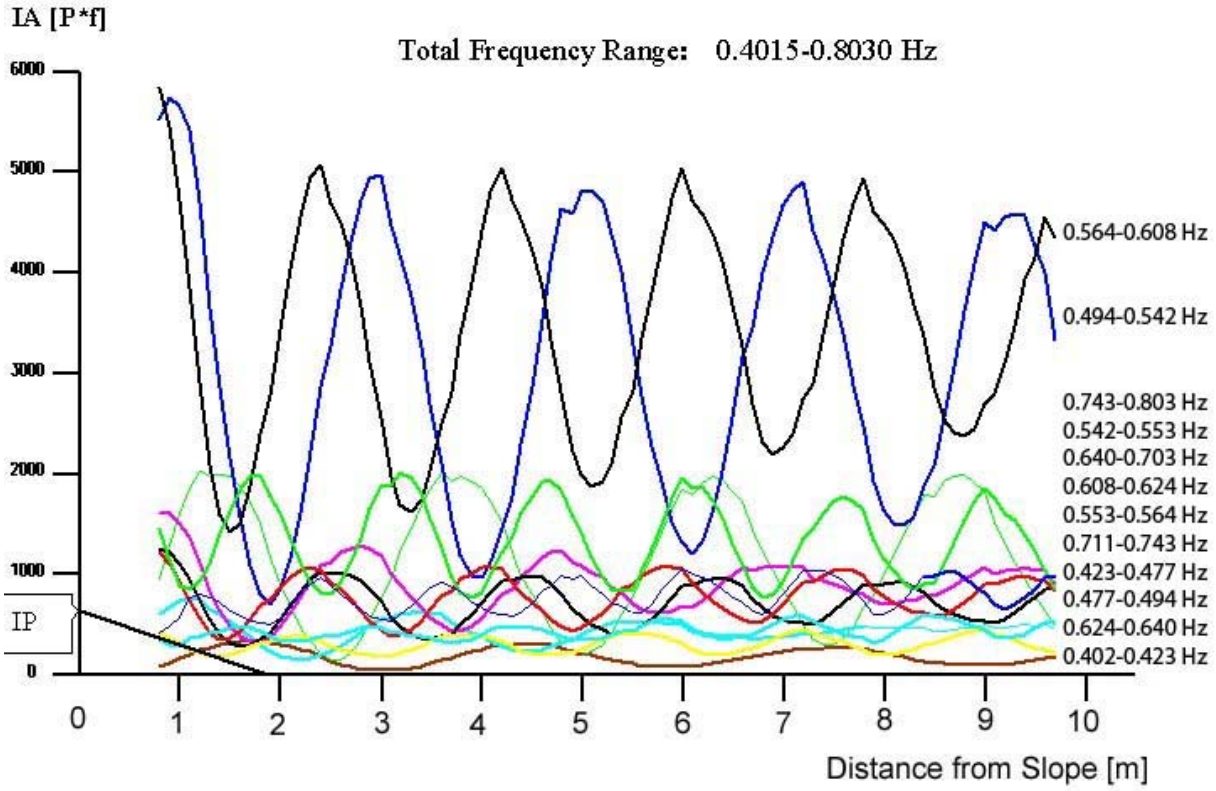

Fig. 06: Energy content of 12 partial standing waves

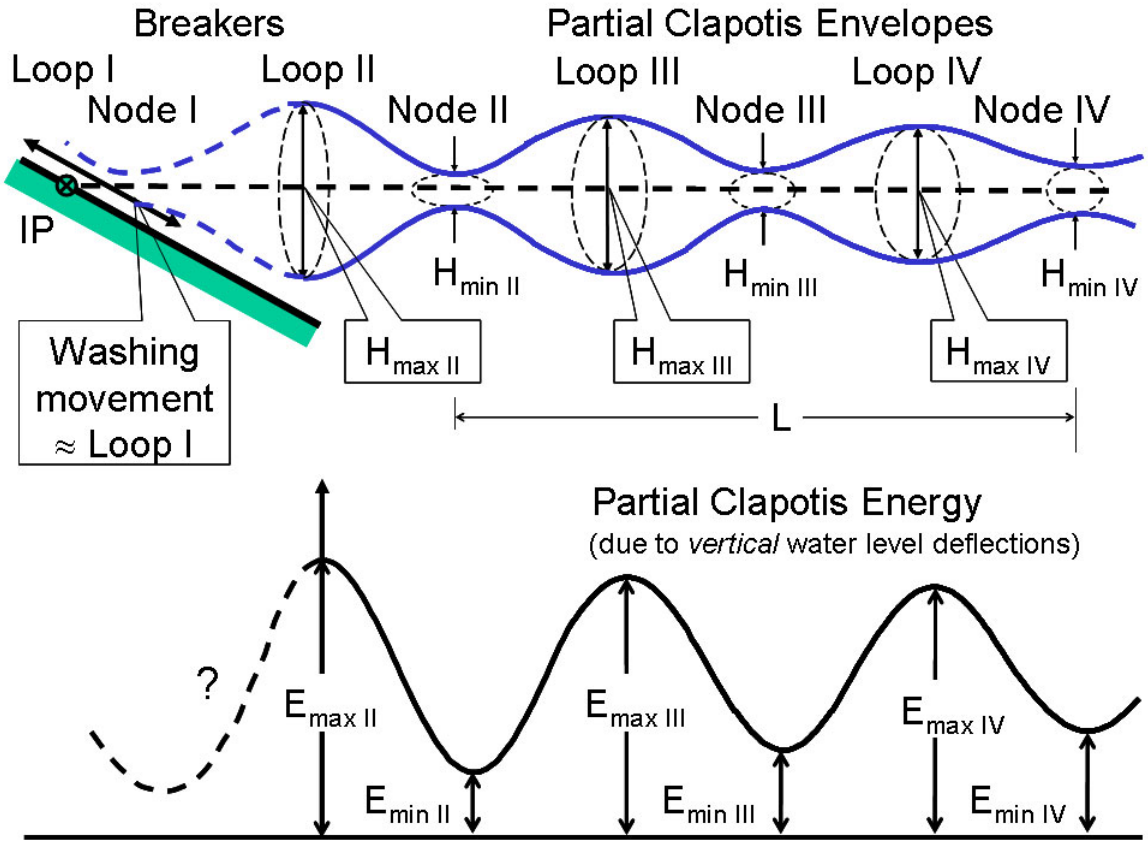

Fig. 07: Sketch of partial standing wave at a slope.

In the lower part of that graph it can be seen that the absolute maximum of energy (denoted E_{maxII}) appears closest to the slope and the seaward maxima E_{maxIII}, E_{maxIV} …decrease in magnitude with the distance increasing from the slope. Vice versa with respect to the curve minima the energy increases with distance from the slope in the order E_{minII}, E_{minIII}, E_{minIV} …
Obviously such features correspond rather well to the water level envelopes of a *partial standing wave* attenuating with distance from IP, as shown in the upper part of Fig.07.
Differing from the periodical potential energy function of a perfect standing wave (clapotis), at which the nodes are related to zero values and the loops to maximum values, obviously at partial standing waves the respective extreme values distinctively deviate from that periodical function. This feature will be discussed further below in chapter 4 with reference to the calculation of reflection coefficients C_r.
Moreover such deviations allow phenomenological explanations with respect to the water particle kinematics as indicated in the graph:
The particle movements at phases of the loops may be approximated by ellipses possessing *bigger vertical* principle axis and those at the node phases by ellipses possessing *bigger horizontal* principle axis. The orbital motions of partial waves *approaching* the slope may be described by *increasing* vertical ellipse axis at the loops and *decreasing* vertical ellipse axis at the nodes.
In the following, previous results are summarized based on the existence of the above energy lines and their properties, on which also will be referred to in the remainder of this paper.

3. Resonant basin oscillations and anomalous dispersion of frequency components of partial standing waves

A comprehensive report on resonant basin oscillations in the wave tank used, is contained in publication [8]. Thus its appearance is due to the generation of wave sequences repeatedly without any precautions to suppress re-reflection from the wave maker.

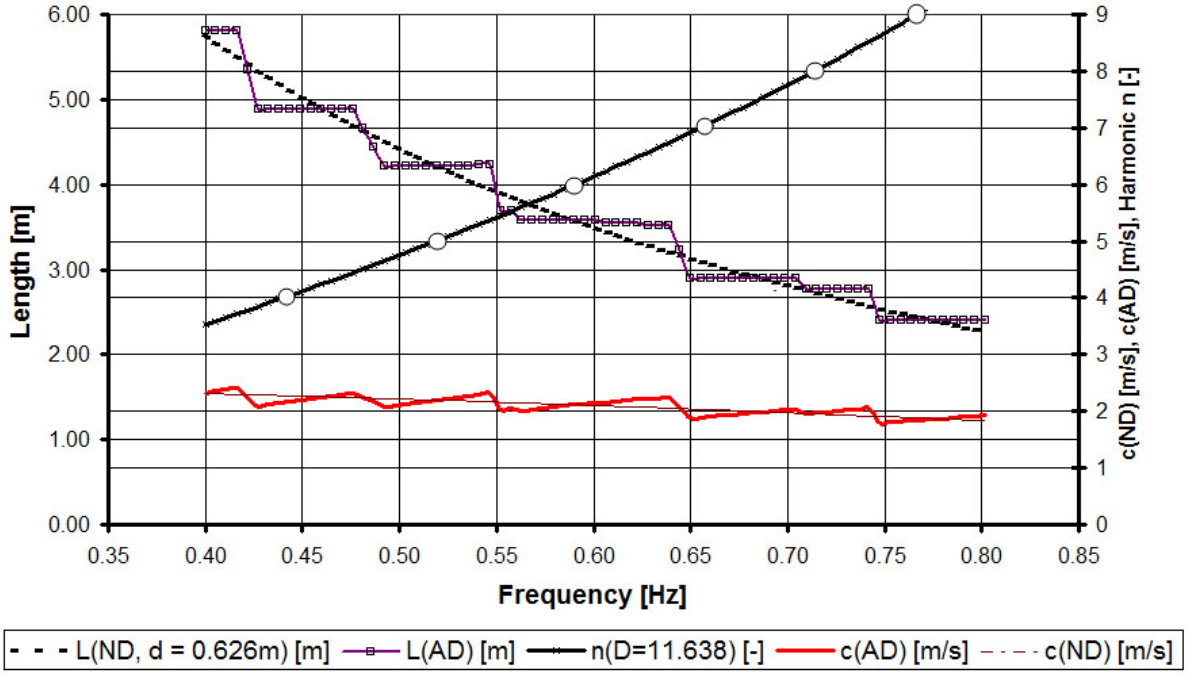

Fig.08: Component length L, phase velocities c and harmonic numbers n plotted with frequency.

The phenomenon of grouping frequency components was shown above in chapter 2. Due to the fact that the frequency components of the partial waves have nearly equal wave length, follows that there is an *anomalous dispersion property* within such wave packets, because the phase velocity according to $c = L \cdot f$ increases with frequency. It is $dc/df > 0$.

In the upper part of Fig.08 the lengths associated with the 82 energy lines, mentioned above, are denoted L(AD)(f) (AD = anomalous dispersion), whereas L(ND)(f) (ND = normal dispersion; dashed line) refers to the *classical dispersion relation* according to water depth d = 0.626 m in the wave tank. Thus, both curves can be named *Length Spectra*. Besides the mentioned (red) phase velocity spectrum c(AD)(f) also the theoretical phase velocity spectrum c(ND)(f), derived from $\omega^2 = g \cdot k \cdot \tanh(k \cdot d)$, is shown in the lower part of the figure.
Especially because of the stepped structure of L(AD)(f), the author considers the 12 partial waves to match the different oscillatory modes of the enclosed water body in the tank.
Hence, the combined appearance of *resonance* and *anomalous dispersion*, known from electromagnetic waves, might also be valid in this case.
In order to confirm this statement the author in [8] previously considered a basin with vertical walls at the front end and at the rear end of a wave tank.
By contrast in the present article, it is shown that the geometry of a basin comprising a vertical wall at the front end and an inclined wall at the rear end provides the appropriate boundary conditions for the function of harmonic numbers of basin oscillations n(f), see Fig.08.
According to the statement, made in the introduction, this function is based on the existence of a node at the slope face and a loop at the wave maker, see Fig.09.

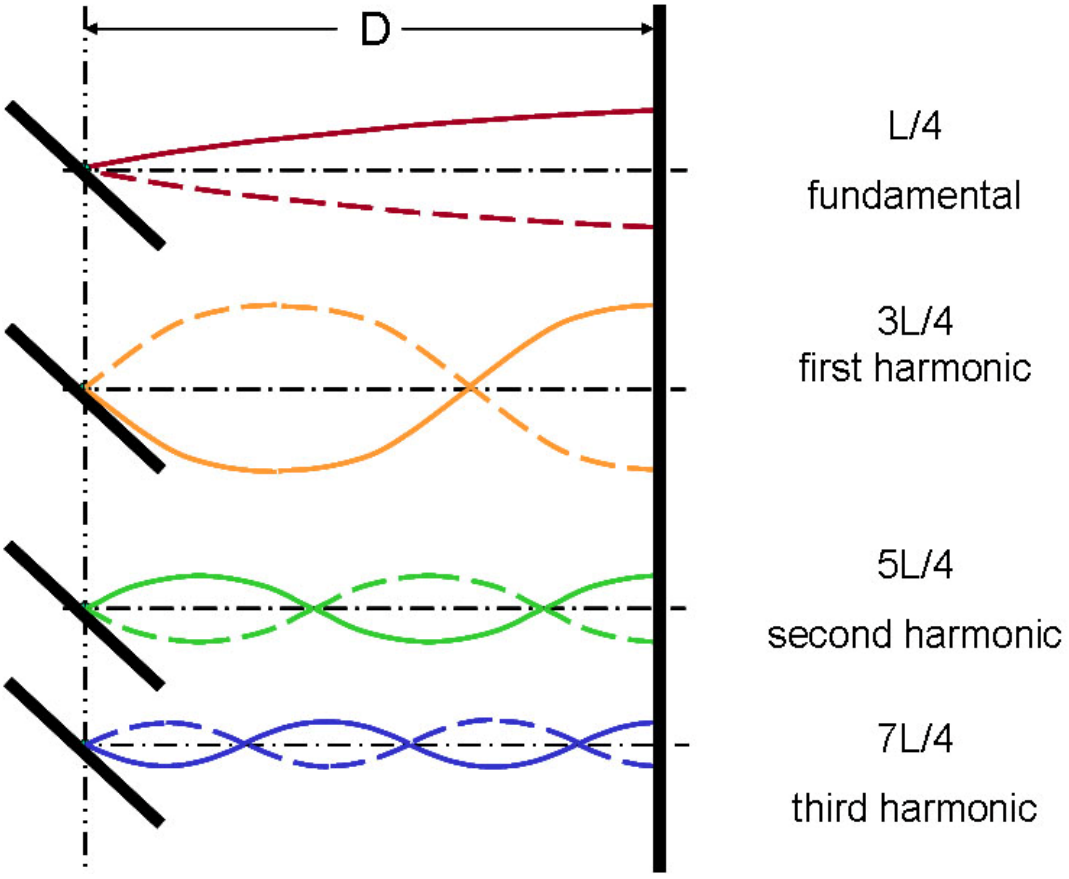

Fig.09: The first 4 theoretical mode shapes of natural oscillations in a basin confined by a vertical wall at the front end and an inclined wall at the rear end.

Natural frequencies of a water volume in a basin comprising of a vertical wall at the front end and an inclined wall at the rear end can be calculated in using formula (03):

$$f\left[Hz\right]=\left(2n+1\right)\cdot\frac{c}{4\cdot D} \qquad (3)$$

where
D = horizontal wall distance according to Fig,09,
c = wave celerity and
n = harmonic number.
n = 0 denotes the fundamental oscillation and n = 1, 2, 3 ... are named first, second, third harmonic etc., Fig.09.

Solving formula (3) with respect to harmonic numbers n[-], yields formula (04):

$$n\left(f\right)\left[-\right]=\frac{2\cdot D\cdot f}{c}-0{,}5 \qquad (4)$$

Further applying c = L · f yields formula (5)

$$n(L)\left[-\right]=\frac{2\cdot D}{L}-0{,}5 \qquad (5)$$

With the horizontal wall distance D = 11.638m (between IP and the hinge of the wave maker) in formula (4), it is evident in Fig.08 that partial waves actually occurred as harmonics of ordinal numbers $4 \le n \le 9$ in the wave tank. It is to be seen that the function is best for the partial waves with wave lengths 3.58m and 4.21m, which both carry maximum energies.

4. Reflection coefficients of partial standing waves and selective reflection of partial waves

One of the authors previous results [9] consisted in the finding that reflection from a sloping structure – whether smooth or hollow – strongly depends on the frequencies contained in the spectrum of gravity waves. Especially the fact that the longer the frequency components, the more down slope they are reflected (to be seen from Fig.06), had been denoted as a kind of *selective reflection.* Such a dependency of course also can be demonstrated by using reflection coefficients.
The calculation of such reflection coefficients $C_{r,i}(f)$ in [3] and [9] formerly had been based on the *structure* of Healy´s formula (1953), but contrary to the sums and differences of wave heights in that formula, here the square roots of the energy extreme values had been used instead as follows:

$$C_{r,i}=\frac{\sqrt{E_{\max,i}}-\sqrt{E_{\min,i}}}{\sqrt{E_{\max,i}}+\sqrt{E_{\min,i}}}. \qquad (6)$$

Where:
Emax,i= maximum energy of contributing components at clapotis loop i,
Emin,i = minimum energy of contributing components at clapotis node i,
i = number of clapotis loops or nodes respectively according to Fig.07.

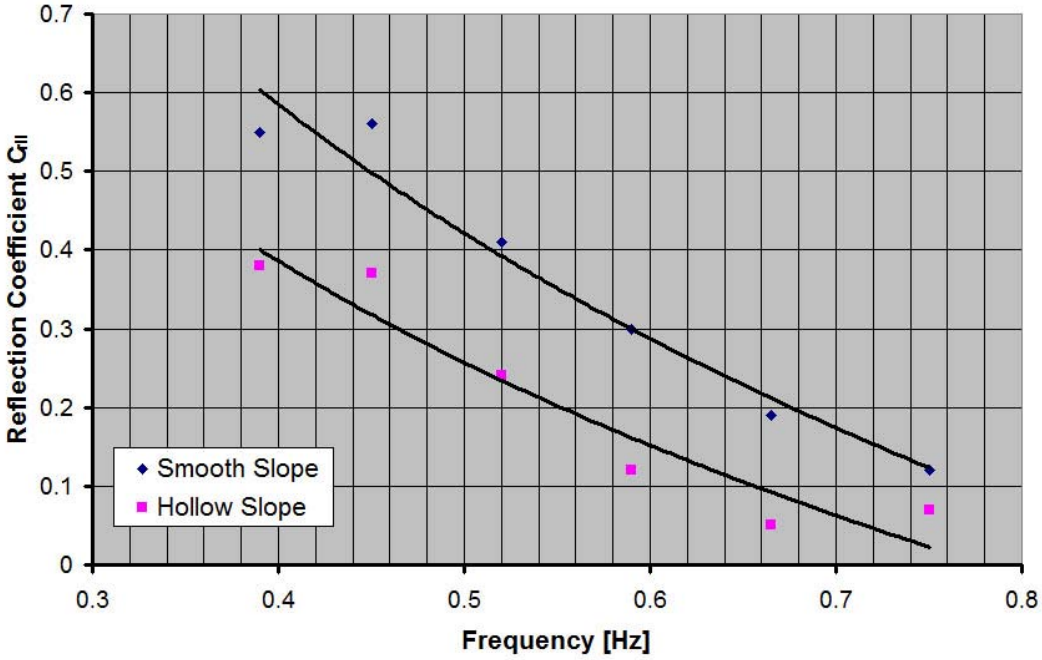

Fig.10: Spectral reflection coefficients $C_{r,II}(f)$ of partial waves at slopes 1:m = 1:3 with mean values of the respective component frequencies f.

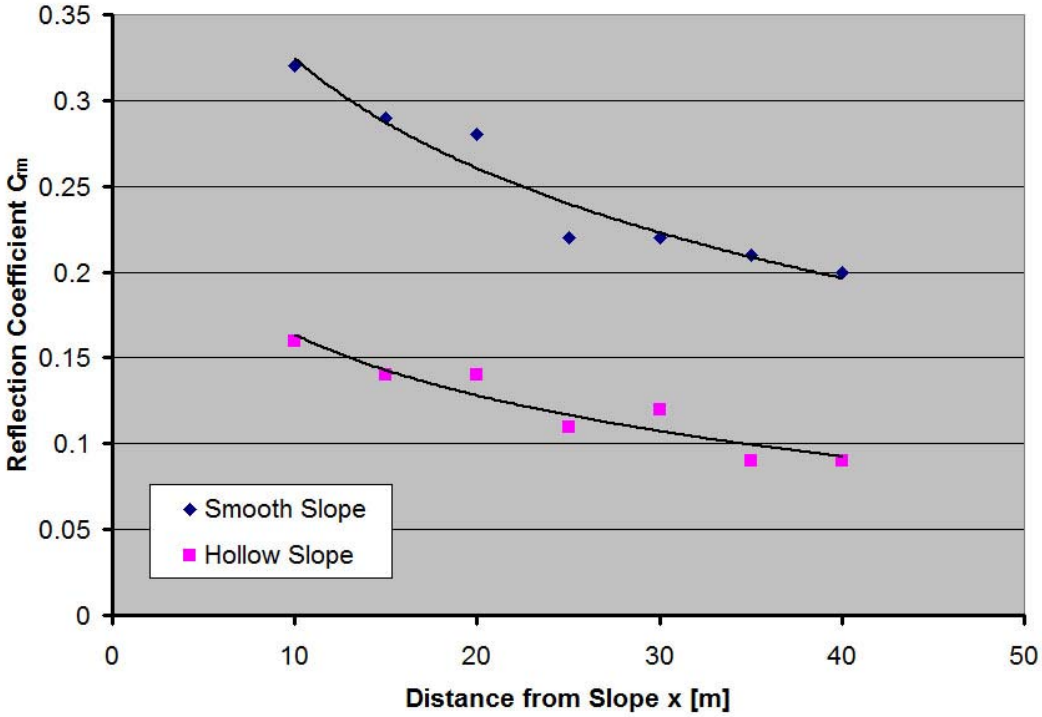

Fig.11: Weighted mean reflection coefficients $C_{r,m}(x)$ of total spectra with prototype distance from a slope 1:3.

There are exemplified plots of the maximum reflection coefficients $C_{r,II}$ (referring to $E_{max,II}$ and $E_{min,II}$) to be seen in Fig.10 for smooth and hollow slopes 1:3 respectively.
But also reflection coefficients $C_{r,m}(x)$, attenuating with distance from the slope, can be presented, which can be useful with regard to safety considerations of ships travelling near a

sloping structure, for instance at the entrance of an harbour. Plots of such reflection coefficients $C_{r,m}(x)$ are to be seen from Fig.11, representing mean values weighted with the energy content of component frequency ranges. Further information on that is contained in [9]. The advantage of the above definitions of reflection coefficients is the fact that the differing mean energy levels in front of the two sloping structures (see Fig.04) are also considered in the evaluation procedure for the reflection coefficients. In this connection it can be questioned, whether *conventionally* calculated reflection coefficients at all can deliver reliable estimates on wave absorption.
Anyhow, in the present case the mean energy levels of the breaker zone close to the sloping structure are related roughly 1: 2/3, cf. Fig. 3 and 4. But it has to be considered here that with respect to the curve, valid for the smooth structure, the *absolute maximum* could not be obtained, because the water depth at stations nearer than 0.79m from IP was not sufficient for measurements to be made. Because this shortcoming is relevant with respect to the relative positioning of partial waves in front of the smooth and the hollow structure, it was necessary to consider additionally the results of similar investigations on the *steeper* slope 1:2, where measurements could be performed nearer to the slope also.

5. Relative phases of partial standing waves at steep slopes and resulting wave deformation

Because of data missing in Fig.07 with respect to the breaking kinematics on the slope face, vague statements are allowed in this context only:

- Energy decreases in upslope direction depending on the type of breaker and on the slope angle.
- The breaker extends from maximum Loop_II and a location near IP.
- Comparing particle movements on the slope to those at a vertical wall, the washing movement on the slope corresponds to Loop_I (directly at the vertical wall face), although the run-up can be compared better to a broken clapotis.

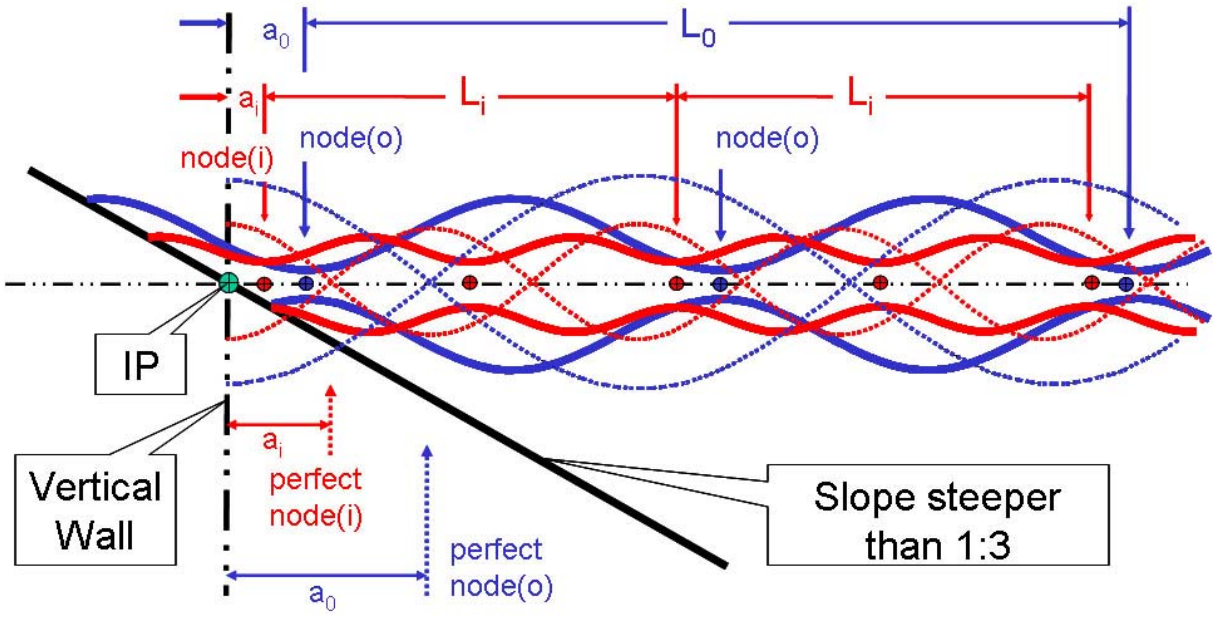

Fig.12: Two sets of partial clapotis of lengths L_0 and L_i at a vertical wall and at a slope 1:m ≥ 1:3 respectively. Vertical wall: dotted lines; Smooth slope: solid lines.

Further statements, however, can be obtained from the relative positioning of the above set of partial clapotis waves (partial waves). For this purpose first of all in Fig.12 some general changes are shown, which occur in the case that a vertical wall is replaced by a sloping structure steeper than 1:3 [10]: Because of the vertical boundary missing, in those cases the perfect nodes convert into approximately elliptical flow lines (spiral shaped imperfect nodes), whose centres are located appreciably nearer to IP than L/4, 3L/4, 5L/4 ….
This is shown here for two sets of wave lengths L_0, L_i at a vertical wall and at a slope respectively.
In the following, evaluations at first are performed with respect to this feature on the smooth slope 1:3, based on the relative distances between the partial clapotis energy lines of Fig.06. Here the longest component partial wave energy line is selected as a reference. This can be identified in the graph by its $E_{minII} \approx 0$ (nearly zero) at 3m from IP. Hence this kind of oscillation (comprising frequencies $0.402 \leq f \leq 0.423$Hz) actually comes rather close to a perfect clapotis.

Pre-breaking Wave Stage

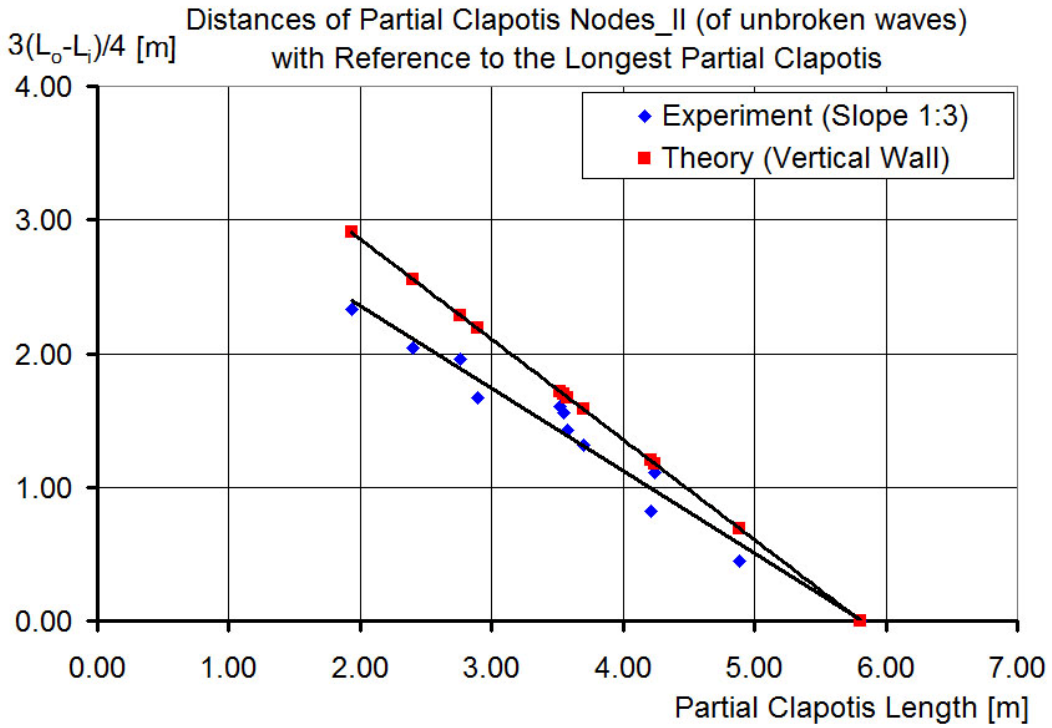

Fig.13: Distances of partial clapotis nodes_II with reference to the longest partial wave of length $L_0 = 5.81$m.

During the process of wave deformation (at a slope) a *pre-breaking wave stage* obviously can be assigned to the position of node_II (3L/4 distant from vertical wall (IP)) of the longest clapotis component. In Fig.06 the respective location (of corresponding minimum energy of frequency components in the range 0.4015 – 0.4232 Hz) is the one mentioned above (3m from IP). The corresponding wave length is equal to the distance between E_{minII} and E_{minIV} resulting in approximately $L_0 = 5.81$m. Hence, in this case (of a slope structure) the distance of the node_II from IP is only about 2L/4 (2.91m) instead of 3L/4 (4.36m). The distances from here to the nodes_II of the remaining component clapotis waves are plotted in Fig.13.
Comparing the results with the respective phase conditions at a vertical wall (theory), it can be seen that those distances decrease with the component frequency increasing (wave length

decreasing). This means that in the *pre-breaking* wave stage the steepening of the resultant wave is due to the relative upsetting of partial clapotis component envelopes.

Breaking Wave Stage

Measurements could not be performed by using wave gauges on the slope face in the water depths region of the *breaking waves,* because of insufficient operational water depth. Hence, in Fig.06 the loops_II (maxima of energy) can be seen for the lower frequency partial wave only. It can, however, be reasonably assumed that at *wave breaking* the process of upsetting partial clapotis components will continue. The loops_II of all clapotis components superimpose in such a way that an asymmetric distribution of energy is produced and stable surface elevations of the resultant waves can no longer be preserved. As to be seen from Fig.04 the asymmetry in the energy distribution with respect to the resultant partial clapotis is preserved also in the seaward wave cycles.

Post-breaking Wave Stage

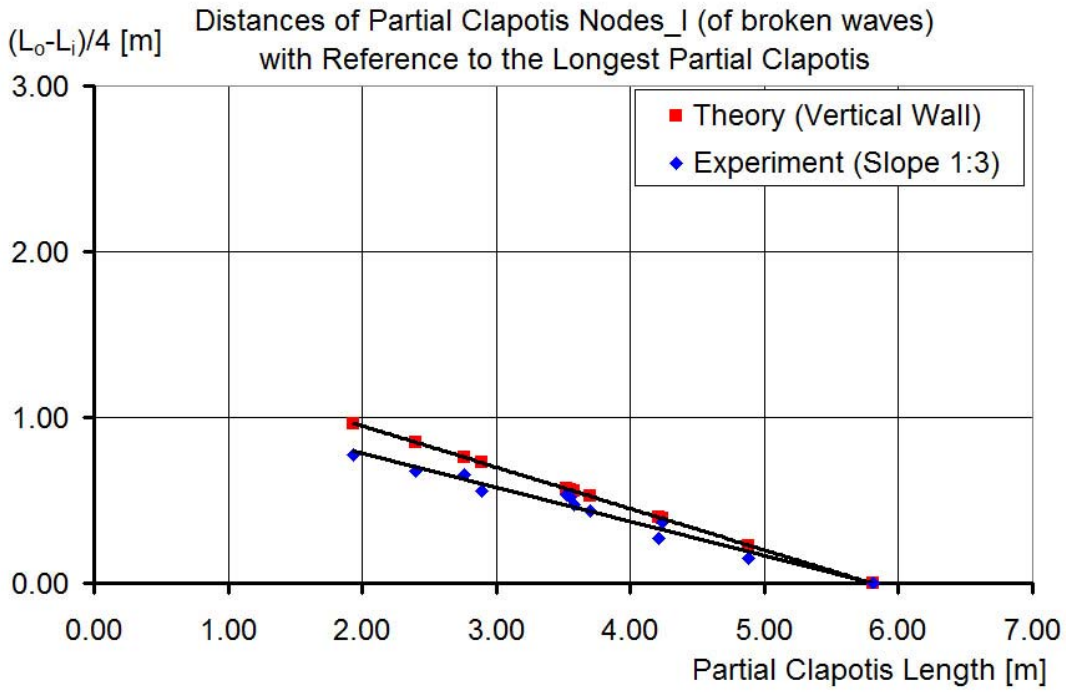

Fig.14: Distances of partial clapotis nodes_I with reference to the longest partial clapotis of length L_0 = 5.81m.

Also the nodes_I (at a distance of L/4 from the vertical wall) of course can *not* be seen directly in Fig.06. Presuming, however, that partial clapotis lengths are constant on the slope, the locations of nodes_I can be extrapolated in using the measured relative distances of the nodes_II, shown in Fig.13. Similar to Fig.13 the extrapolated *relative* distances of clapotis nodes_I with reference to those at a vertical wall (theory) are plotted in Fig.14. As the vertical scale is the same as in Fig.13, it is apparent that differences here are much smaller. This is also an indication that asymmetry changes with the shifting of clapotis components. The absolute clapotis_I node distances a_i from IP, as defined in Fig.12, are shown in Fig.15 and the relative clapotis_I node distances a_i/L_i with reference to IP in Fig.16.

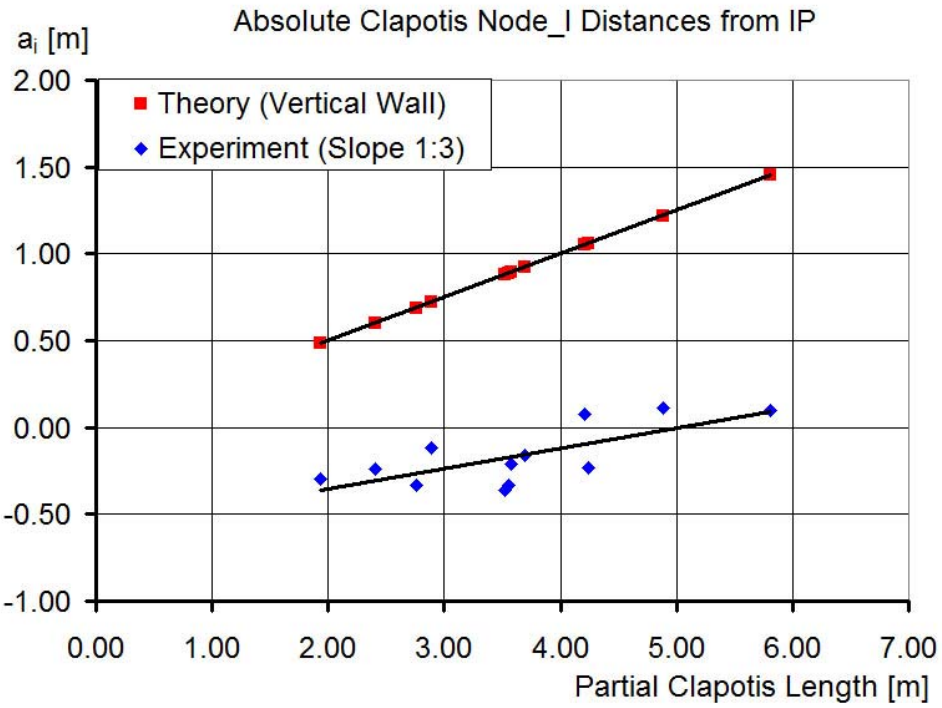

Fig.15: Absolute clapotis node_I distances from IP nearest to the slope face.

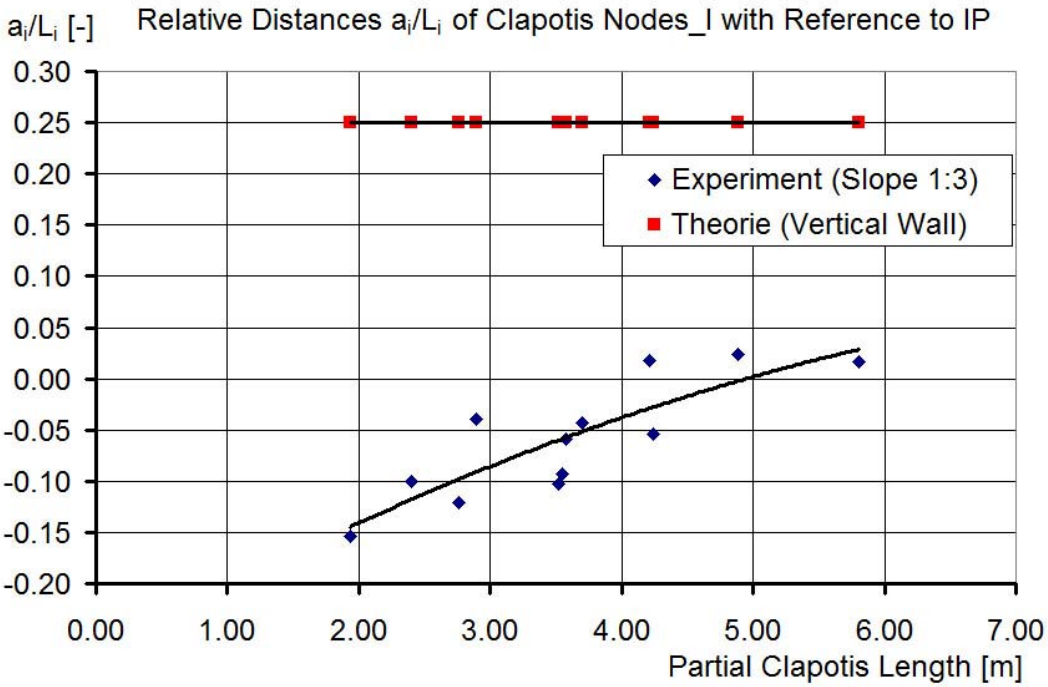

Fig.16: Relative clapotis node_I distances with reference to IP.

It can be seen that the nodes_I are shifted the more in the upslope direction, the higher the partial clapotis frequencies are. The negative values in Fig.15 and Fig.16 are plausible, because water particle movements extend in the upslope direction beyond IP and thus an increasing SWL - well known as wave setup - must exist.

On the other hand the relative shifting of the nodes can also be explained by the kinematics of the incident waves, whose longer (lower-frequency) components are more effected by the boundary of the slope (at bigger water depth) than the shorter (higher-frequency) ones.
Anyhow, a position of node_I close to the slope can be documented for any partial wave. This statement holds even for the maximum deviations from IP, because they are negative and thus on the upslope side.
With respect to the waves resulting from the superimposition of the set of partial waves, it may be stated, that the breaker steepness, besides increasing wave heights, is due to decreasing wave lengths too.
The shifting of the nodes by 90º ($\pi/2$) onto the slope, however, would be of elementary importance, because this means a phase jump of 180º between incident and reflected waves, cf. chapter 6.
In contrast, extrapolating the experimental curve in Fig.16 by the multiple of the maximum examined wave length, would trend to the limiting value $a_i/L_i = 0.25$. Hence, extremely long waves actually would tend towards the status of a clapotis without a phase jump.
Similar results had been published by the author previously in [10] and for monochromatic waves also in [3].
Because of a better judgment of the above results for the smooth slope and supposed deviations for the hollow slope, in the following similar results on slopes 1:m = 1:2 are included in the analysis. The hollow structure in this case, however, is rather different from that of Fig.01. As to be seen from Fig. 17, in this case two layers of big hollow cubes had been piled up in such a way that a stepped structure is formed, see also [11 and 12].

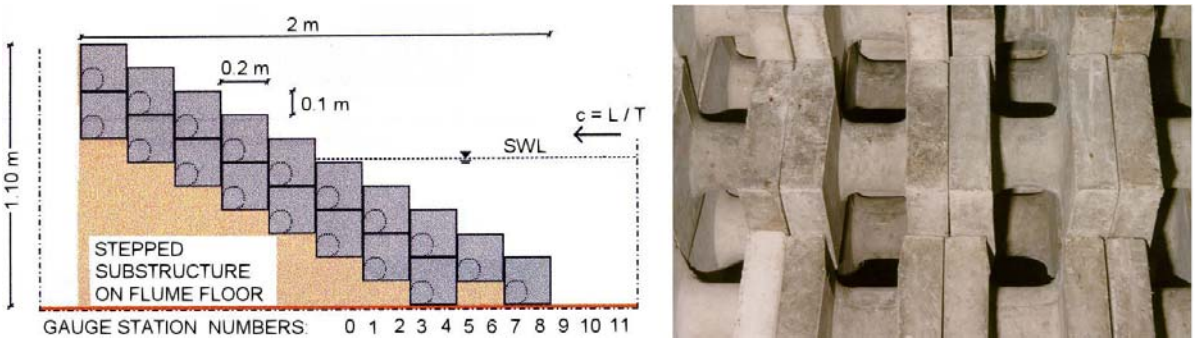

Fig.17: Sectional and cut-out views of test structure composed of "Hollow Cubes".

The results for this structure and for the respective smooth reference slope are contained in Fig.18. Actually the measuring procedure here was similar to that one used for the slope 1:3, but the method of presenting the data is different to that one used for Fig.06.
Instead of plotting the data of any partial wave separately, in this case the energy contents of all partial waves, comprising different component frequency ranges, appear piled up with reference to the distance from IP. The energy values of each partial wave are marked by colors to be identified from the inset at the bottom of the graph.
Additionally it has to be mentioned here that truncated wave sequences had been applied in such a way that the re-reflection effect was excluded from the analyzed data and accordingly measurements extend about 3m from IP only.
Provided that signal noise of frequencies $f > 0.725$ Hz is disregarded, (i.e. the upper yellow-orange areas in both plots) at the smooth slope partial waves can very well be identified by their extreme values of energy representing loops and nodes respectively.[1] Moreover the

[1] The distinct increase of energy within the frequency range $0.6 \leq f \leq 0.68125$Hz at station 5 may be traced back to unknown local wave breaking features not to be discussed here.

"selective reflection effect" mentioned above, is very distinct: The lower the frequency components of a partial wave the more down-slope they are reflected with the consequence of the relative shifting to be seen in the graph. Thus actually the nodes_I appear rather close to IP except for the longest two partial waves comprising the frequency range 0<f<0.375Hz. It should be mentioned here that at slopes 1:2 measurements could be performed yet close to IP.

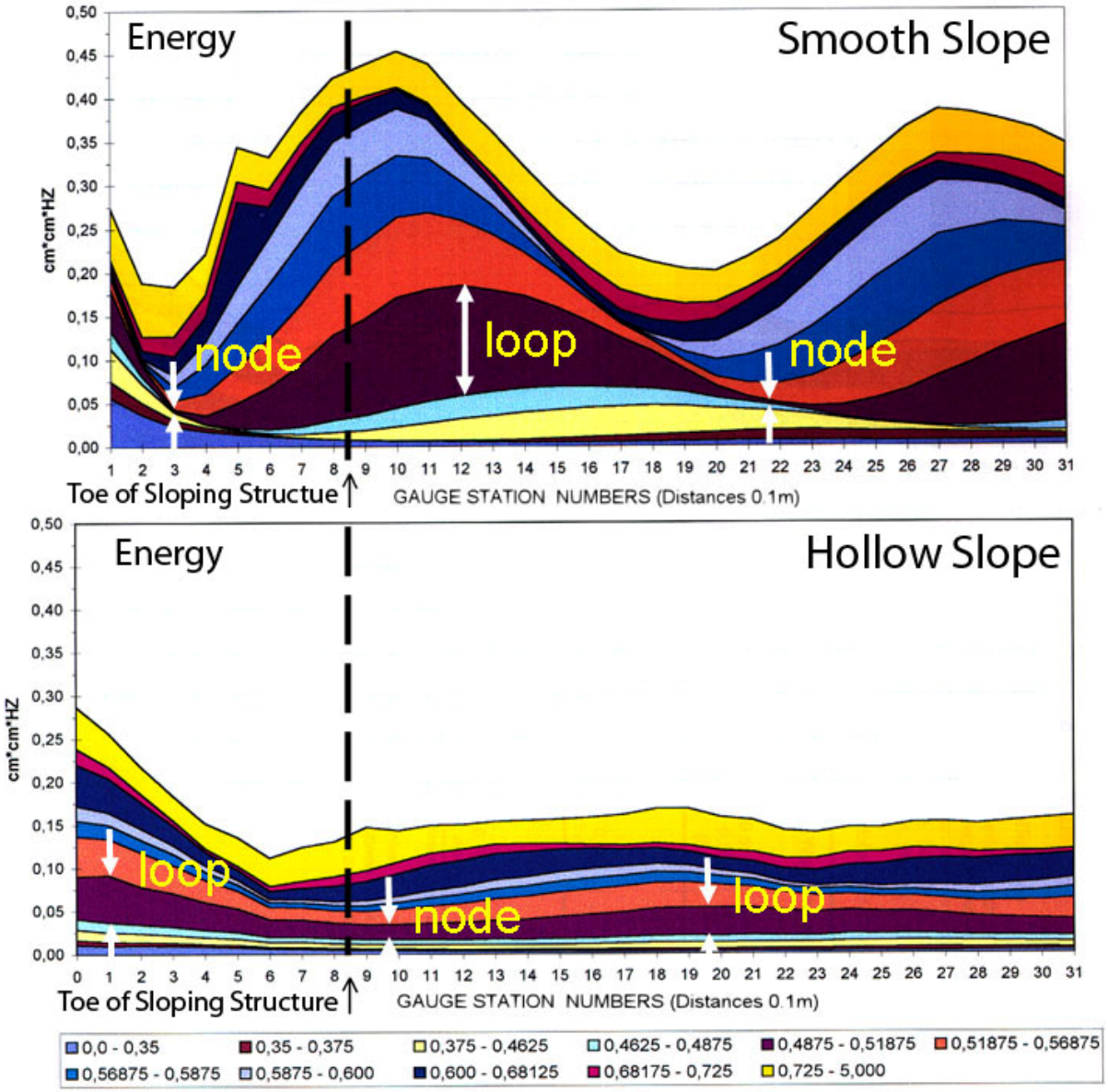

Fig.18: Smooth slope: Evidence of partial waves with extreme values of energy documenting distinct loops and nodes.
Hollow Structure: Evidence of partial waves with much less energy.
Distinct phase differences between respective partial waves at both slopes.

Apparently at the hollow structure the loops and nodes are much less distinct, but still can be identified. Comparing, however, the energy contents of the respective partial waves in front of the two slopes, the differences not only of the magnitudes but also of the phases are impressive. The distances of corresponding partial wave phases can be taken from the graph. By way of example with regard to the frequency range $0.4875\text{Hz} \le f \le 0.51875\text{Hz}$, whose loops and nodes in the graph are marked by arrows, the distance of corresponding phase

points is 0.70m. Applying 0.95m as the distance between node and loop (also taken from the graph) the phase difference can easily be figured out to be $\Delta\psi = 66°$.[2]

With regard to reflection coefficients (to be further analyzed in chapter 7), estimates depending on frequency, calculated in using the above method, are shown yet in Fig.19. Hence, in the frequency range $0.36\text{Hz} \le f \le 0.7\text{Hz}$ there are reflection coefficients $0.5 \le C_r \le 0.85$ attached to the smooth slope and $0.1 \le C_r \le 0.3$ to the hollow structure.

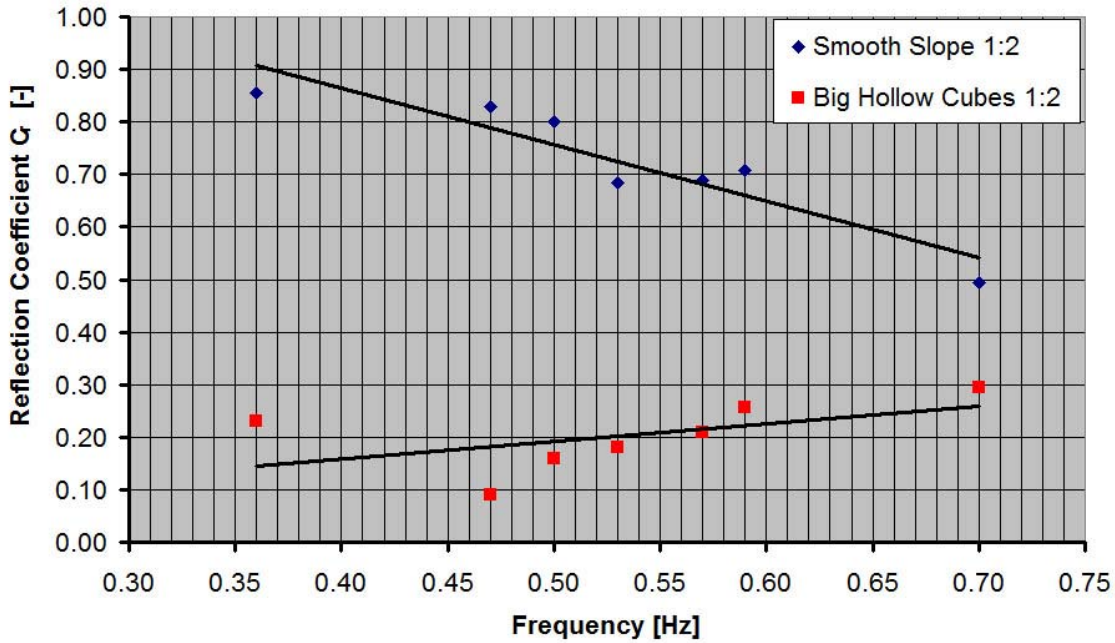

Fig.19: Spectral reflection coefficients $C_{r,II}(f)$ of partial waves at slopes 1:m = 1:2 plotted with the mean values of corresponding frequency ranges.

Similar to Fig.10 reflection coefficients for the smooth slope decrease with frequency increasing. Contrary the trend of coefficients for the hollow structure is rather neutral.
In contrast to the smooth slope, above the hollow structure, there is a loop documented between stations 5 and 0 due to increasing energy, see Fig.18. This increase is, however, combined with a shifting of energy from lower frequencies $0 < f < 0.46875\text{Hz}$ to higher frequencies $0.4875\text{Hz} < f < 0.725\text{Hz}$ and is in accordance with the visual observation of high turbulent flow into and out of the hollow structure respectively.
Thus it can be supposed that besides energy dissipation at the hollow structure, also the magnitude of the observed phase difference is responsible for the very low reflection coefficients to be found. By contrast, at a slope 1:3 a comparable phase difference is only $\Delta\psi = 18° < 66°$ attached to a similar frequency range $0.49\text{Hz} \le f \le 0.54\text{Hz}$. Although the reduction of reflection coefficients is impressive for the hollow revetment 1:3 (Fig.10) also, the collapsing breaker occurring at that structure is rather different from surf characteristics at the hollow structure inclined 1:2.

[2] In the same frequency range, the minimum energy value at station 6 may be traced back to the impermeable in-place step to be seen from Fig.17. This can also not be discussed here.

6. Further considerations on the occurrence of a phase jump between incident and reflected waves.

In the 1990ies the author had already mentioned the interaction process between the washing movement on the slope face and the particle movement, induced by the incident waves, with the consequence of a possible resonance between them [1]. Naturally for this purpose not only the matching of the frequencies is important but also the relative phases of both movements. In this connection special relevance may be attached to the *position* of the partial clapotis in front of the sloping structure. In the following it will be shown that the position of the later depends on the phase difference between incident and reflected wave.
In case that - differing from the conventional treatment - the reflected wave is distinguished not only by a wave height $H_r < H_i$ but also by a different phase φ with respect to the incident wave, an appropriate reflection coefficient $C_r = f(H_r/H_i, \Delta\varphi)$ can be specified for *cosine waves* by way of a parametric representation.[3] In doing so the function $C_r = f(\Delta\varphi)$ had been calculated for parameters $0.1 \le H_r/H_i \le 1.0$, where individual values for given phase differences Δφ come from Healy´s formula (1953).

$$C_r = \frac{H_{max} - H_{min}}{H_{max} + H_{min}} \quad \text{where } H_{max} = H_i + H_r \text{ and } H_{min} = H_i - H_r \qquad (7)$$

For the *theoretical* case of two opposing cosine waves of equal wave length (or period) an example of the calculation scheme for the parameter $H_r/H_i = 0.7$ and phase difference $\Delta\varphi = \pi/4$ is contained in Fig.20.

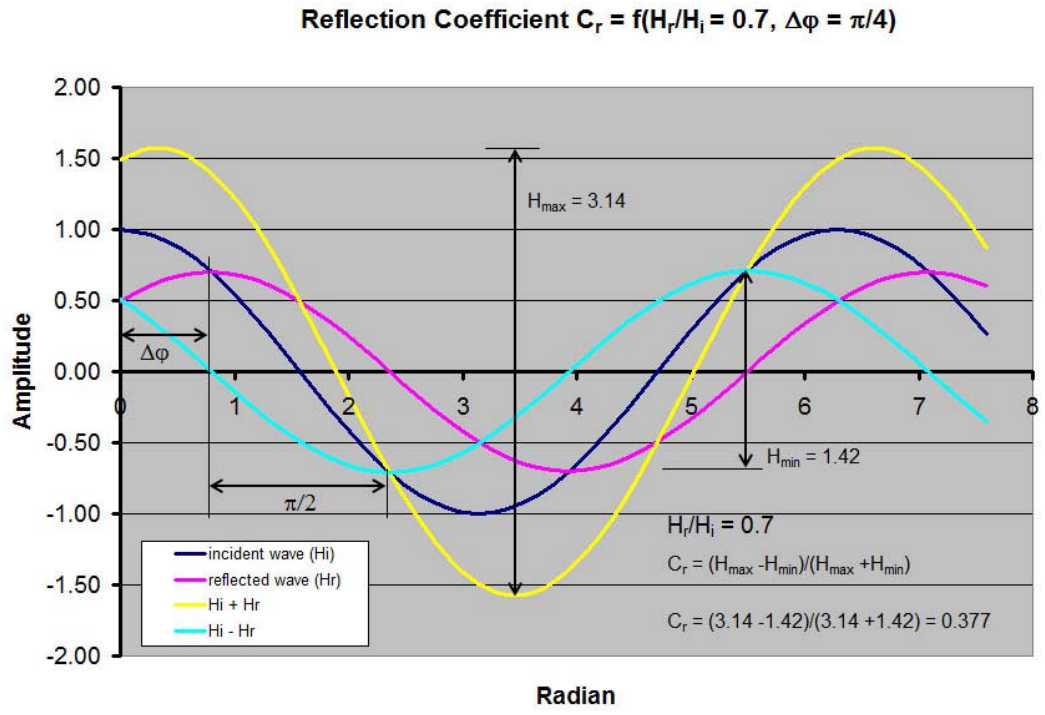

Fig.20: Calculation scheme for reflection coefficient $C_r = f(H_r/H_i = 0.7; \Delta\varphi = \pi/4)$

As shown in the graph the phase difference Δφ produces a displacement of the partial clapotis, whose loops and nodes are characterized by the extreme values of the functions H_{max} and

[3] A complex reflection coefficient may be formulated alternatively.

H_{min}. Additional consideration of the phase distance $\Delta\varphi$ in this case causes a change of the reflection coefficient from $C_r = f(H_r/H_i) = 0.7$ to $C_r = f(H_r/H_i, \Delta\varphi) = 0.377$.
The entirety of reflection coefficients $C_r = f(H_r/H_i, \Delta\varphi)$ for parameters $0.1 \le H_r/H_i \le 1.0$ and phase differences $0° \le \Delta\varphi \le 180°$ is plotted in Fig. 21. Outside this range reflection coefficients can be found by mirroring the data at the axis $\Delta\varphi = 0°$ and at the axis at $\Delta\varphi = 180°$ respectively.
It should be noted here that due to the used definition in this presentation *negative* reflection coefficients are found for phase distances $90° < \Delta\varphi \le 180°$.
Considering at first the theoretical case of equal cosine wave heights $H_i = H_r$ (curve parameter $H_r/H_i = 1$), the reflection coefficient $C_r = 1.0$ at $\Delta\varphi = 0°$ is attached to a perfect clapotis comprising of a loop at the point of reflection (e.g. at a vertical wall), whereas the phase difference $\Delta\varphi = 180°$ delivers a negative reflection coefficient $C_r = -1.0$.

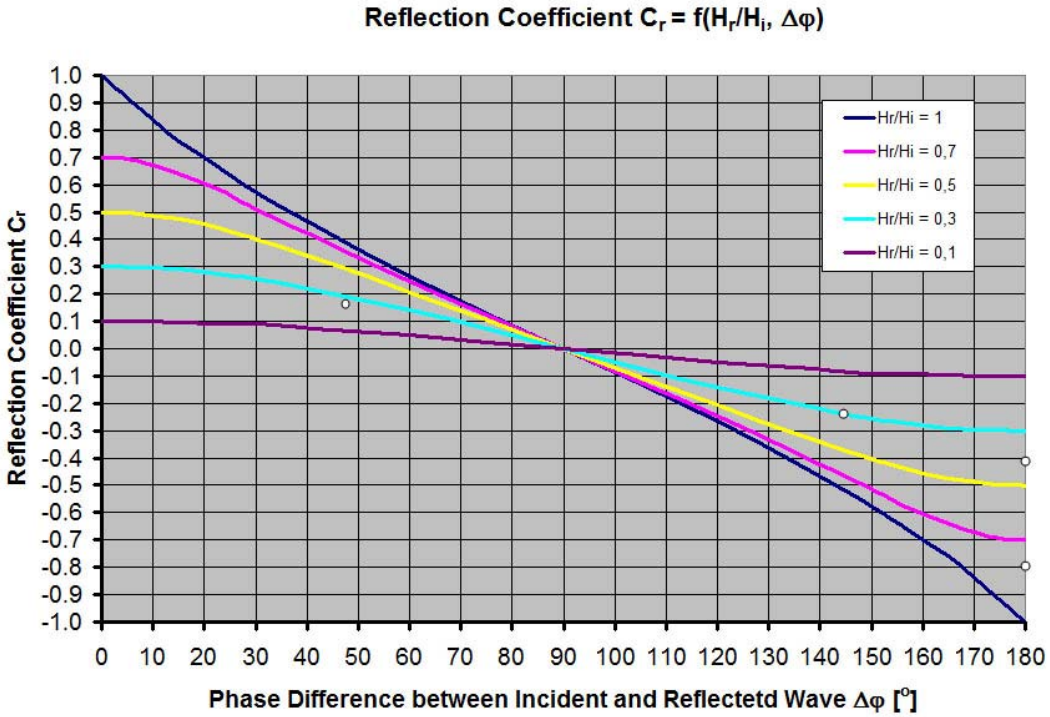

Fig.21: Reflection coefficients $C_r = f(H_r/H_i, \Delta\varphi)$ in the range of parameters $0.1 \le H_r/H_i \le 1.0$ and phase distances $0° \le \Delta\varphi \le 180°$.

The later, however, also stands for a perfect clapotis, but in this case with a *perfect node* existing at the point of reflection and thus a phase jump is produced.
Considering both of the clapotis waves separately apart from their originating incident and reflected waves, their loops appear shifted by an angle of $\Delta\phi = 90°$ ($\pi/2$).
Accordingly for $\Delta\varphi$ changing from 0° to 180°, the transfer from the case of *reflection without phase jump* to the case of *reflection with phase jump* can be watched, meaning that the wave crest is reflected as a wave trough and vice versa.
At the phase difference $\Delta\varphi = 90°$ there is $C_r = 0$, i.e. no reflection exists.
Phase differences $0° < \Delta\varphi < 90°$ and $90° < \Delta\varphi < 180°$, however, represent partial standing waves, which can be considered a mixture of progressive and standing waves. In those cases imperfect nodes are located at distances $0 < a_i < L_i/4$ from IP.
Of course there are also partial standing waves at phase differences 0° and 180°, if parameter $H_r/H_i < 1$.

Hence, the general conclusion to be drawn from Fig.21 consists in the statement that a phase difference between incident and reflected wave reduces the magnitude of the reflection coefficient the more the closer it is to 90° (π/2).
Determining reflection coefficients from the envelopes of partial standing waves or from the above energy lines respectively, thus it is important to decide, which kind of partial clapotis really exists. So, according to the investigations on hand, one should act on the assumption that there exists negative reflection at the two smooth slopes 1:3 and 1:2 with *mean* reflection coefficients $C_r \approx -0.35$ (Fig.10) and $C_r \approx -0.75$, (Fig.19) respectively.
Also imperfect negative reflection would exist at the hollow slope 1:3, expressed by the mean reflection coefficient $C_r \approx -0.2$, (Fig.10), while there is imperfect positive reflection at the hollow structure inclined 1:2 with a mean reflection coefficient $C_r \approx +0.2$ (Fig.19), due to the imperfect loop close to IP (see Fig18).
A quantitative statement on how much the phase difference $\Delta\varphi$ is responsible for the excellent result with this kind of hollow structure, is given exemplarily for a selected frequency range in chapter 7.
Contrary without any information on the positioning of the partial clapotis with reference to IP, the reflection coefficient would be ambiguous. This is indicated e. g. for a value $C_r = 0.2$ and phase differences $0° \leq \Delta\varphi \leq 90°$ by the markers on the curves in the lower part of Fig.22.

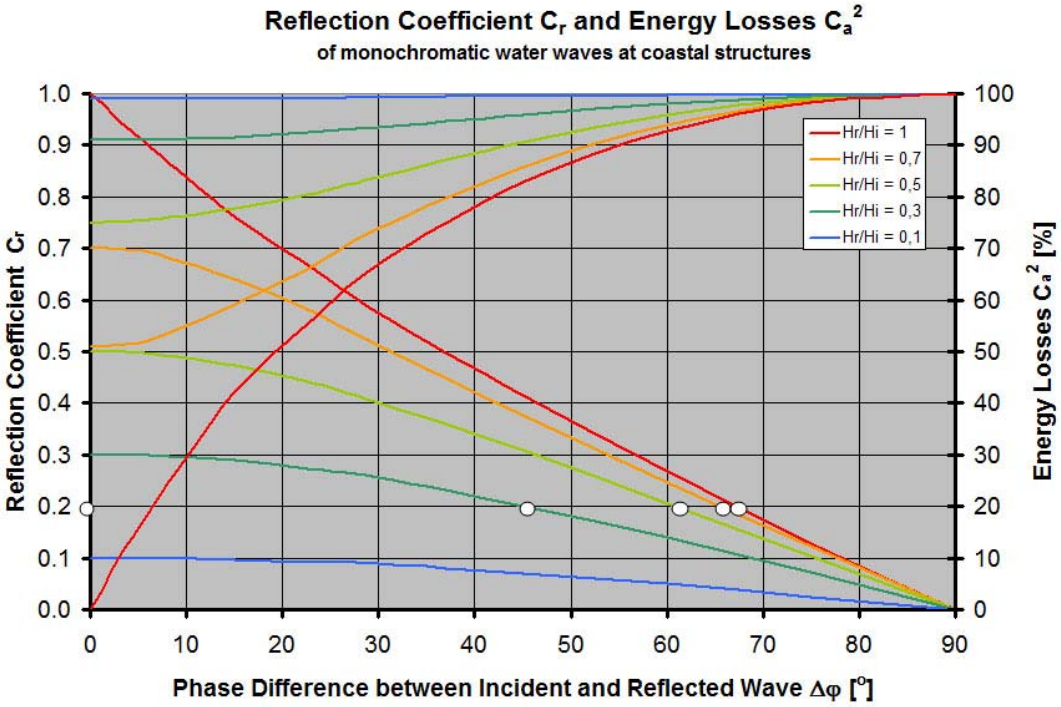

Fig.22: Lower Family of Curves: Reflection coefficients $C_r = f(H_r/H_i, \Delta\varphi)$; Upper Family of Curves: Absorption loss $C_a^2 = f(H_r/H_i, \Delta\varphi)$.

In the present case of non-inundated structures the linkage between reflection coefficient C_r and absorption coefficient C_a is normally established based on the energy conservation law as follows:
The energy of incident waves E_i is equal to the sum of reflected energy E_r and absorbed energy E_a.

$$E_i = E_r + E_a \qquad (8)$$

With reference to the phenomenological model of wave breaking, specified in the introduction, it has to be clarified at this place that the fraction of reflected energy E_r is originated right during the process of wave breaking and the fraction of absorbed energy E_a

comprises the total energy dissipation at breaking *and* at further interaction with the sloping structure, though the breaking process itself is induced by the structure.

As wave energy is proportional to the square of the wave height, follows

$$H_i^2 = H_r^2 + H_a^2 \qquad (9)$$

and division by H_i^2 delivers the relationship between the coefficients squared, substituting the respective energy fractions.

$$1 = C_r^2 + C_a^2 \qquad (10)$$

Hence the upper family of curves in Fig.22 comprises the absorption losses

$C_a^2 = 1 - C_r^2 = f(H_r/H_i, \Delta\varphi)$.

Simply it is shown here that according to the overall decrease of reflection coefficients (lower family of curves) with phase difference in the range $0° \leq \Delta\varphi \leq 90°$ there is an increase of the absorption losses up to 100%.

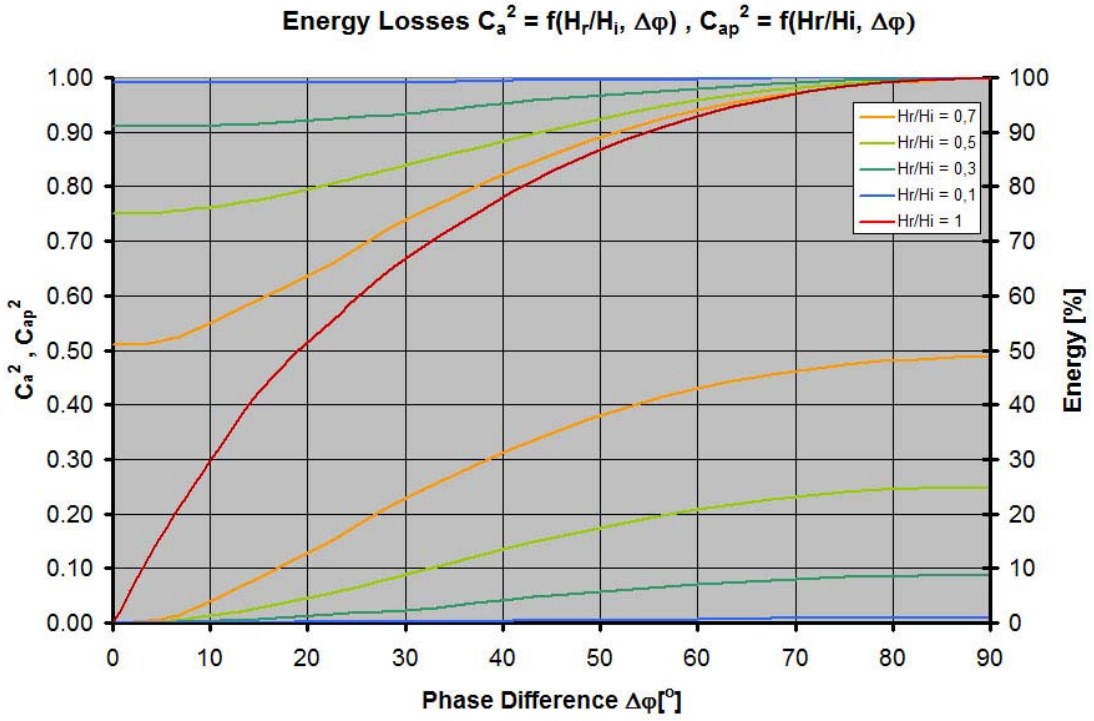

Fig.23: Upper Family of Curves: Total absorption loss $C_a^2 = f(H_r/H_i, \Delta\varphi)$. Lower Family of Curves: Fraction of absorption loss $C_{ap}^2 = f(H_r/H_i, \Delta\varphi) = C_a^2 - C_a^2(\Delta\varphi=0)$ due to phase difference.

In order to (further) clarify the effect of the phase difference, in Fig. 23 the total absorption loss $C_a^2 = f(H_r/H_i, \Delta\varphi)$ is contrasted by the *rate* of absorption loss $C_{ap}^2 = f(H_r/H_i, \Delta\varphi) = C_a^2 - C_a^2(\Delta\varphi=0)$ (lower family of curves), which will result, if $C_{a0}^2 = C_a^2(\Delta\varphi=0)$ is subtracted from the former.

Thus in the case of $H_r/H_i = 0.7$ e.g. the phase difference $\Delta\varphi = 90°$ causes nearly half (49%) of the total absorption loss. The phase difference $\Delta\varphi = 30°$, however, produces a balance as follows:

$$C_r^2 + C_{a0}^2 + C_{ap}^2 = 26\% + 51\% + 23\% = 100\% \qquad (11)$$

Then in this case the rate of absorption due to the phase difference (23%) is approximately equal to the reflected energy (26%), while absorption due to the ratio of wave heights is about twice that of the former two (51%).

7. Estimates of the Phase Difference Δφ Influencing the Reflection Coefficient $C_r = f(H_r/H_i, \Delta\varphi)$

In the following estimates of the influencing values H_r/H_i and Δφ on the reflection coefficient $C_r = f(H_r/H_i, \Delta\varphi)$ are presented basing on Fig.21 and on particular results mentioned above.
In doing so, reference is made to partial waves of frequency range $0.48\text{Hz} \le f \le 0.56\text{Hz}$ for slopes 1:3 and to partial waves of similar frequency range $0.4875\text{Hz} \le f \le 0.518750\text{Hz}$ for slopes 1:2.
In the present case the initial condition of a phase jump (according to a phase difference $\Delta\varphi = 180°$ between incident and reflected waves) may be accurate enough for *both* smooth slopes. Hence negative reflection exists for slope 1:3 with a reflection coefficient of $C_r \approx -0{,}41$ (see Fig.10 and marker in Fig.21) and for slope 1:2 with a reflection coefficient $C_r \approx -0{,}8$ (see Fig.19 and marker in Fig.21).
Provided that phase jumps $\Delta\varphi < 180°$ also at partial reflection cause a node shift of $\Delta\phi = \Delta\varphi/2$, the node shifts $\Delta\psi$, to be taken from evaluations analog to Fig.18, can be attached to phase differences Δφ as follows:
The node shift related to the point of origin is $\Delta\phi = 90° - \Delta\psi$.

Hence $\Delta\varphi = 2(90° - \Delta\psi)$. (12)

With the reflection coefficient $C_r = f(H_r/H_i, \Delta\varphi)$ known from a proper evaluation scheme, the parameter H_r/H_i can be found from the family of curves of Fig.21 to be the curve running through point $P(\Delta\varphi, C_r)$.

As for the *hollow slope 1:3*, the node shift between the respective partial waves is $\Delta\psi = 18°$ leading to a phase difference $\Delta\varphi = 144°$.
Together with $C_r = f(H_r/H_i, \Delta\varphi) = -0.24$ (Fig.08) follows $H_r/H_i \approx 0.30$ (see marker in Fig.21). Hence the absolute reduction due to phase shift contained in the reflection coefficient is 0.30-0.24 = 0.06 or 20%.
As for the *hollow structure 1:2*, the node shift between the respective partial waves is $\Delta\psi = 66°$ leading to a phase difference $\Delta\varphi = 48°$.
Together with $C_r = f(H_r/H_i, \Delta\varphi) = +0.17$ (Fig.19) follows $H_r/H_i \approx 0.26$ (see marker in Fig.21). Hence the absolute reduction due to phase shift contained in the reflection coefficient is 0.26-0.17 = 0.09 or about 35%.

8. Conclusions (Hypothesis and Further Observations)

The above findings especially with reference to Fig.21 are giving cause to a hypothesis "On the Reflection of Partial Standing Waves at Inclined Sloping Faces".
Contrary to the perfect standing wave at a vertical wall due to retro-reflection *without a phase jump* (i.e. positive reflection characterized by a node distance a = L/4 from the wall; $C_r = 1.0$; $\Delta\varphi = 0^o$) there is another kind of retro-reflection *with a phase jump* at a wall inclined by a certain angle (i.e. negative reflection characterized by a node at the reflecting wall; $C_r = -1.0$; $\Delta\varphi = 180^o$). Both types of clapotis should be considered as theoretical limiting cases of reflection excluding any friction effects at interfaces (water – air and water – solid respectively).

Moreover cases of *partial reflection* characterized by $C_r = f(H_r/H_i = 1; 0^o < \Delta\varphi < 180°)$ should be labelled as theoretic too, provided that energy dissipation processes not only exhibit a change of the reflected wave height but also a change of the reflected wave phase.
All the remaining cases of partial reflection, however, with parameters $0 < H_r/H_i < 1$ and $0^o < \Delta\varphi < 180^o$ are due to different kinds of energy dissipation processes.
With respect to the shapes of breaking waves, it can be supposed in this context that not only the Iribarren number for surf similarity $\xi = \tan\alpha/\sqrt{(H/L)}$ but also the phase difference $\Delta\varphi$ may be adequately important.
At least at the steep slopes treated here, comprising smooth or nearly smooth surfaces, there exists a negative reflection, which, however, needs further specification with respect to the slope angle.
The distinct negative reflection effect can be attached most probably to surging waves, but may also be responsible for the plunging breaker type to occur. Moderate negative reflection occurred at hollow slopes producing collapsing breakers, while there was no distinct breaker type to be identified at big hollow cubes accounting for very low positive reflection coefficients.

9. References

[1] BÜSCHING, F.: Durchströmbare Böschungsstrukturen, Bauingenieur 66, S. 11-14, 1991
[2] SCHOEMAKER, H.J. AND J.TH. THIJSSE: Investigation of the reflection of waves, Third Meeting, Intern. Assoc. Hyd. Structures Res., 1-2 September, 1949
[3] BÜSCHING, F.: Hollow Revetment Elements 1. Proc. Fourth International Conference on Coastal and Port Engineering in Developing Countries COPEDEC IV, Rio de Janeiro, S. 961-976, 1995. 2. Beiträge aus dem Küsteningenieurwesen (Papers on Coastal Engineering), FH Bielefeld, Abt. Minden, Nr. 4, 1996
[4] SUTHERLAND , J. AND O'DONOGHUE, T.: Wave Phase Shift at Coastal Structures, Journal of Waterway, Port, Coastal and Ocean Engineering, Vol. 124, No. 2, March/April 1998, pp. 90-98.
[5] BÜSCHING, F.: On Energy Spectra of Irregular Surf Waves, Proceedings, 15th Internat. Conference On Coastal Eng., Honolulu, Hawaii, USA, 21 Seiten, 1976
[6] BLEES, O. UND STÜHMEIER, M.: Wellen und Strömungen vor geböschten Uferschutzbauwerken, Diplomarbeiten FH Bielefeld University of Applied Sciences 1991, unveröffentlicht
[7] HAGEMEYER, K. UND KRAMER, M.: Reflexion irregulärer Wellen an geböschten Uferschutzbauwerken, Diplomarbeiten FH Bielefeld University of Applied Sciences 1992, unveröffentlicht
[8] BÜSCHING, F.: Sturmwellen-Resonanz an der Westküste der Insel Sylt, Die Küste, Heft 67, 2003 pp. 51-82.
[8] Büsching, F: Wave Resonances Detected in a Wave Tank and in the Field, Ocean Wave Measurement and Analysis, 5th Int. Symposium Waves 2005, Madrid, Spain, Paper number: 134, 12pp.
[9] BÜSCHING, F.: Wave and Downrush Interaction on Sloping Structures, Proc. 10th International Harbour Congress, Antwerpen, S. 5.17-5.25, 1992
[10] BÜSCHING, F.: Combined Dispersion and Reflection Effects at Sloping Structures
1. 4th International Conference on Coasts, Ports and Marine Structures, ICOPMAS´2000, Proceedings (Abstracts and CD), Bandar Abbas, Iran, 21. – 24. Nov. 2000.
2. International Conference on Port and Maritime R&D and Technology ICPMRDT, p.411-418, Singapore, 29.-31.10.2001, Proc. / CD

[11] BÜSCHING, F.: Hollow Cubes – Durchströmbare Hohlformkörper als Bauelemente wellenbelasteter Böschungsabdeckungen - HANSA –International Maritime Journal - C 3503 E, 138, H. 10 p.62-65, 2001.
[12] BÜSCHING, F.: Reflection from Hollow Armour Units, Proc. COPEDEC V, p.1362 - 1370, Cape Town, South Africa 1999.
[13] LEMKE, S. UND NICOLAI, A.: Reflexion an einer aus Beton-Hohlformkörpern (Hollow Cubes) bestehenden Böschung mit der Neigung 1:2, Diplomarbeit FH Bielefeld University of Applied Sciences, 1998, unveröffentlicht.
[14] KOBAYASHI, N., TOMASICCHIO, G.R AND BRUNONE, B.: Partial Standing Waves on a steep Slope, Journal of Coastal Research, 16(2), 2000, 379-384, ISSN 0749-0208.
[15] BÜSCHING, F.: 2010. Phasensprung bei der partiellen Reflexion irregulärer Wasserwellen an steilen Uferböschungen, 1. HANSA –International Maritime Journal ISSN 0017-7504, C 3503 E, 147, H. 5 p.87-98, 2010. 2. Binnenschifffahrt ISSN 0939-1916, C 4397 D, 65, H.9 p.73-77 & H.10, p. 64-69.